Enhanced wintertime oxidation of VOCs via sustained radical sources in the urban atmosphere

Sommariva, Roberto; Crilley, Leigh R.; Ball, Stephen M.; Cordell, Rebecca L.; Hollis, Lloyd D.J.; Bloss, William J.; Monks, Paul S.

DOI:
10.1016/j.envpol.2021.116563

Enhanced wintertime oxidation of VOCs via sustained radical sources in the urban atmosphere

Roberto Sommariva[a,b,*], Leigh R. Crilley[b,1], Stephen M. Ball[a], Rebecca L. Cordell[a], Lloyd D. J. Hollis[a], William J. Bloss[b], Paul S. Monks[a]

[a] *Department of Chemistry, University of Leicester, Leicester, UK*
[b] *School of Geography, Earth and Environmental Sciences, University of Birmingham, Birmingham, UK*

Abstract

Daytime atmospheric oxidation chemistry is conventionally considered to be driven primarily by the OH radical, formed via photolytic sources. In this paper we examine how, during winter when photolytic processes are slow, chlorine chemistry can have a significant impact on oxidative processes in the urban boundary layer. Photolysis of nitryl chloride ($ClNO_2$) provides a significant source of chlorine atoms, which enhances the oxidation of volatile organic compounds (VOCs) and the production of atmospheric pollutants.

We present a set of observations of $ClNO_2$ and HONO made at urban locations in central England in December 2014 and February 2016. While direct emissions and in-situ chemical formation of HONO continue throughout the day, $ClNO_2$ is only formed at night and is usually completely photolyzed by midday. Our data show that, during winter, $ClNO_2$ often persists through the daylight hours at mixing ratios above 10-20 ppt (on average). In addition, relatively high mixing ratios of daytime HONO (>65 ppt) provide a strong source of OH radicals throughout the day.

The combined effects of $ClNO_2$ and HONO result in sustained sources of Cl and OH radicals from sunrise to sunset, which form additional ozone, PAN, oxygenated VOCs, and secondary organic aerosol. We show that radical sources such as $ClNO_2$ and HONO can lead to a surprisingly photoactive urban atmosphere during winter and

*Corresponding author
Email address: rs445@le.ac.uk (Roberto Sommariva)
[1]Present address: Department of Chemistry, York University, Toronto, Canada

should therefore be included in atmospheric chemical models.

Keywords: nitryl chloride; nitrous acid; chlorine; OH radical; tropospheric ozone

---

Highlights

- High $ClNO_2$ concentrations at sunrise cause it to persist until sunset above 10-20 ppt
- Daytime HONO accounts for over 90% of OH formation in the winter urban atmosphere
- Sustained sources of Cl and OH throughout the day enhance the oxidation of VOCs
- Production of O_3 and secondary pollutants increases and continues into the afternoon

1. Introduction

The oxidation of volatile organic compounds (VOCs) in the lower atmosphere leads to the formation of ozone (O_3), secondary organic aerosol (SOA) and other harmful pollutants (e.g. aldehydes, PAN) via a complex series of chemical reactions initiated by reactive radical species. The current understanding of oxidative processes in the troposphere is that the most important daytime oxidant is the hydroxyl radical (OH). However, chlorine atoms (Cl) are being increasingly recognized as important tropospheric oxidants (Simpson et al., 2015; Sherwen et al., 2017; Wang et al., 2019), although chlorine chemistry is often not included in the air quality models used for regulatory purposes. Because of their high reactivity, Cl atoms can considerably accelerate the oxidation rate of VOCs above that of OH chemistry alone, thus increasing the formation of secondary atmospheric pollutants.

The dominant source of the OH radical across the troposphere is the photolysis of ozone, followed by the reaction of excited state oxygen atoms (O^1D) with water vapour (Figure 1). Ambient studies have shown that the reactions of ozone with unsaturated VOCs (alkenes, dialkenes, terpenes) and the photolysis of nitrous acid (HONO) can be more important primary sources of OH than ozone photolysis, especially in the urban boundary layer (Emmerson et al., 2005; Ren et al., 2006; Kanaya et al., 2007; Elshorbany et al., 2009; Lee et al., 2016; Tan et al., 2018; Slater et al., 2020). Because of its relatively short photolysis lifetime (in the order of tens of minutes), HONO has long been considered as a significant OH source, mainly during the morning. However, more recent field studies have found non-negligible HONO concentrations in urban environments during the day, which suggest that there are significant daytime sources of HONO (Kleffmann, 2007; Villena et al., 2011; Michoud et al., 2014) and, therefore, that the influence of HONO on radical production may be more extensive than previously thought. Besides the gas-phase reaction OH + NO, important sources of HONO are direct emissions, e.g. from vehicles (Kurtenbach et al., 2001; Kramer et al., 2020) and from microbial activity in the soil (Su et al., 2011). In addition, HONO is known to be formed via heterogeneous reactions of NO_2 on humid surfaces both during the night and during the day (Finlayson-Pitts et al., 2002; Vogel et al., 2003; Spataro

and Ianniello, 2014). Photo-enhanced conversion of NO_2 into HONO has been observed in laboratory studies on several surfaces, with organic films the most productive (Ammann et al., 1998; George et al., 2005; Stemmler et al., 2006), and has also been observed on "urban grime" on building surfaces (Baergen and Donaldson, 2016) and on snow in urban environments (Chen et al., 2019; Michoud et al., 2015). The relative contribution of urban daytime sources of HONO is an active area of research, with models still largely unable to account for measured daytime concentrations (e.g. Michoud et al. (2014); Lee et al. (2016)).

Cl atoms are released into the gas phase via a number of different mechanisms (Simpson et al., 2015): for example, acid displacement of HCl from aerosol and various multi-phase chemical processes that form gas-phase BrCl and Cl_2, followed by photolysis and/or reaction with OH. One mechanism that has recently gathered much attention is the nocturnal formation of nitryl chloride ($ClNO_2$) via reaction of dinitrogen pentoxide (N_2O_5) on chloride-containing aerosol (Figure 1). The photolysis of $ClNO_2$ after sunrise forms Cl atoms and nitrogen dioxide (NO_2), thus increasing the oxidation of VOCs and reducing the loss of NO_x via the nocturnal formation of HNO_3 (Figure 1). The combination of Cl reactivity and higher NO_2 concentrations results in enhanced ozone production – up to 10 ppb of additional O_3 compared to scenarios without $ClNO_2$ chemistry (Osthoff et al., 2008; Sarwar et al., 2014; Tham et al., 2016). Several studies have reported $ClNO_2$ nocturnal mixing ratios ranging from a few tens of ppt to several ppb (e.g. Osthoff et al. (2008); Mielke et al. (2011); Phillips et al. (2012); Riedel et al. (2012); Bannan et al. (2015); Wang et al. (2016)). Depending on the season and meteorological conditions, the photolysis lifetime of $ClNO_2$ at midday in the mid-latitudes can vary between 50 minutes and 3 hours. This means that, typically, over 95% of the nitryl chloride present at sunrise is photolyzed before 11:30 (summer) or 13:00 (spring/autumn), and that most of the direct effect of chlorine reactivity on the formation of atmospheric pollutants takes place during the first few hours of the morning (Thornton et al., 2010; Phillips et al., 2012; Haskins et al., 2019).

In general, the chemical processes that form pollutants in the boundary layer during winter have received less attention than during other seasons, especially under polluted urban conditions. Wintertime chemistry is characterized by lower temperatures, less

intense sunlight and shorter daylight hours, all of which affect the main sources of oxidants, most of which are photolytic. Therefore, the formation of secondary atmospheric pollutants is slower during winter, and any additional source of oxidants, such as Cl atoms, can have a significant impact on urban air quality. Only a few studies have reported $ClNO_2$ observations in wintertime, with nocturnal mixing ratios of the order of several hundreds of ppt (Thornton et al., 2010; Mielke et al., 2016; Priestley et al., 2018; Sommariva et al., 2018; Haskins et al., 2019; McNamara et al., 2020). In these studies, $ClNO_2$ mixing ratios usually fell below the respective instrumental detection limits (in the order of a few ppt) around midday, with the exception of Priestley et al. (2018) who observed $ClNO_2$ mixing ratios $>$4 ppt up until $\sim$15:00 in November in Manchester (UK).

In this paper, we present a dataset of $ClNO_2$ and HONO observations made during winter in an urban environment in central England (UK). On approximately half of the days, $ClNO_2$ remained above the instrument detection limit (4.2 ppt) for the entire daylight period. With the help of a box-model, we show how the persistence of $ClNO_2$ through the daylight hours of winter, combined with the daytime formation of HONO, leads to significantly higher concentrations of radical species (OH and Cl) in the urban boundary layer, and thereby enhances the oxidation of VOCs and the production of secondary pollutants, such as ozone, oxygenated VOCs, PAN and SOA.

2. Materials and Methods

2.1. Instruments

Nitryl chloride ($ClNO_2$) was measured using a Chemical Ionization Mass Spectrometer (CIMS). The instrument (THS Instruments LLC, USA) was operated in negative ion mode using iodide ions (I^-) as the reagent ion, and $ClNO_2$ was detected at m/z = 208, 210 amu, corresponding to the $[I \cdot ClNO_2]^-$ ion cluster (Sommariva et al., 2018). Molecular chlorine (Cl_2) was also measured by CIMS at m/z = 197, 199, 201 amu, which correspond to the $[I \cdot Cl_2]^-$ ion cluster. The inlet line, a 5 m long PFA tube (OD = 3/8”), was regularly washed with deionized water during the measurements to avoid formation of $ClNO_2$ from particles deposited inside the inlet: there was no significant difference in the CIMS signals before and after the line was washed. To calibrate

the CIMS, nitryl chloride was synthetized using a humidified flow of Cl_2 (5 ppm in N_2) over a bed of sodium nitrite ($NaNO_2$) and sodium chloride (NaCl) as described in Thaler et al. (2011): $ClNO_2$ was then quantified via thermal decomposition to Cl and NO_2 (at $\sim$350 °C) followed by measurement of NO_2 by Broadband Cavity Enhanced Spectroscopy (Thalman et al., 2015). Molecular chlorine was calibrated by known dilutions of a 5 ppm certified gas standard (BOC plc, UK). The $ClNO_2$ and Cl_2 detection limits were 4.2 and 7.1 ppt, respectively (2σ, 1 minute).

The CIMS instrument was deployed at the University of Leicester campus, together with a O_3 monitor, a NO_x monitor (T400 and T200, Teledyne Technologies Inc, USA) and a spectral radiometer (MetCon GmbH, Germany) to measure the photolysis rates of over 40 species, including O_3, HONO and $ClNO_2$. Meteorological information (wind speed and direction, temperature, pressure, humidity) was available from the Automatic Urban and Rural Monitoring Network (AURN). The AURN site is located on the University campus and is classed as "urban background".

Nitrous acid (HONO) was measured using a Long Path Absorption Photometer (LOPAP-03, QUMA Elektronik & Analytik GmbH, Germany). As described in Heland et al. (2001), the LOPAP is a wet chemical technique where gas-phase HONO is sampled within a stripping coil into an acidic solution where it is derivatized into an azo dye. Absorption of light at 550 nm by the azo dye is measured with a spectrometer (Ocean Optics Inc, USA) with an optical path length of 2.4 m. The LOPAP sampling unit is a temperature controlled (15-20 °C) box containing a quartz inlet (length $<$5 cm) connected to the main instrument via a 3 m umbilical line that carries the reagents and the azo-dye. The instrument was operated and calibrated according to the standard procedures described in Kleffmann and Wiesen (2008). The HONO detection limit was 0.2 ppt (2σ, 30 seconds).

The LOPAP instrument was deployed at the University of Birmingham campus; Leicester and Birmingham are two cities in central England $\sim$80 kilometers apart. In both locations, the sampling points on the respective University campuses are comparable "urban background sites".

2.2. *Box-model*

A simple box-model was used to investigate the formation of radicals (OH and Cl), the oxidation of VOCs and the production of secondary pollutants. The model was built using AtChem2 v1.2 (Sommariva et al., 2020) with a chemical mechanism taken from the Master Chemical Mechanism (MCM v3.3.1, Saunders et al. (2003); Jenkin et al. (2003)). The chemical mechanism includes a complete inorganic chemistry scheme plus the oxidation mechanism of the 31 VOCs, including methane, that are routinely measured at the AURN sites (Table 1).

Production of HCl from chlorine reactions with VOCs, and production of Cl from the HCl + OH reaction and from $ClNO_2$ photolysis, are not included in the MCM and were added to the mechanism. The chlorine gas-phase mechanism in the model is very simple and does not include inorganic reactions such as $Cl + O_3$, $Cl + HO_2$ and $Cl + O_2$. For the mixture of CH_4 and VOCs listed in Table 1, calculations show that the dominant reaction of Cl atoms is with organics (over 85%), and thus we do not expect the model's omission of Cl inorganic reactions to significantly affect the conclusions of this work The uptake of N_2O_5 on aerosol and the heterogeneous formation of $ClNO_2$ were not included in the mechanism, because the model was only run from sunrise to sunset, when $ClNO_2$ formation is not active. Heterogeneous formation of HONO was also not included, because the model was constrained to the average diurnal profile of measured HONO. The model was constrained to the average diurnal profiles of measured jNO_2, jHONO and $jClNO_2$, while the photolysis rates of the other species in the mechanism were calculated by AtChem2 and scaled to jNO_2.

The model was initialized with the average values observed at sunrise in Leicester during winter 2014 and 2016 (Sommariva et al., 2018) for $ClNO_2$ and other inorganic species (O_3, NO, NO_2, CO) as well as for temperature, relative humidity and pressure. Since measurements of VOCs were not available in either Leicester or Birmingham, the model was initialized with the average VOC concentrations measured during winter at the nearest suburban background AURN site, London Eltham. The initial conditions of all chemical species and physical parameters in the box-model are listed in Table 1.

3. Results and Discussion

3.1. Observations of daytime $ClNO_2$: sources and sinks

The nitryl chloride measurements presented here were part of a larger project aimed at assessing the spatial and temporal variability of $ClNO_2$ in the UK (Sommariva et al., 2018). In this paper, we focus on two wintertime measurement periods in Leicester (52°38' N, 01°08' W), a city in central England ∼200 km from the ocean – the major source of Cl-containing aerosol (sea-salt). $ClNO_2$ was observed above the instrument detection limit every night between 11 and 19 December 2014, and on 19 out of 26 nights between 1 and 26 February 2016. Since the measurements were taken in different years, they are shown in this paper as monthly diurnal averages (Figure 2); the whole dataset and timeseries of the observations are shown and discussed in Sommariva et al. (2018).

During both measurement periods, the peak $ClNO_2$ concentrations were observed at night between 00:00 and 04:00. The mean and median peak mixing ratios were 76 ppt and 50.5 ppt, respectively, in December 2014, and 162 ppt and 139 ppt, in February 2016 (Sommariva et al., 2018). These mixing ratios are consistent with previous wintertime observations of $ClNO_2$ (Thornton et al., 2010; Mielke et al., 2016; Priestley et al., 2018; Haskins et al., 2019). Closer inspection of the dataset revealed two cases, hereafter referred to as highCL and lowCL (Figure 2). On 63% of the days in December 2014 and on 38% of the days in February 2016, $ClNO_2$ concentrations persisted above the instrument detection limit throughout the daylight hours (case highCL), increasing again after sunset (∼16:00 in December, ∼17:00 in February). The lowest diurnal concentrations during these days were observed around 14:00 (in December) and 15:00 (in February), with mean mixing ratios of 10.1 ppt and 20.5 ppt, respectively. On the rest of the days, $ClNO_2$ mixing ratios dropped below the instrument detection limit of 4.2 ppt between 11:00 and 13:00 (case lowCL), similar to what has been observed in prior wintertime studies (Thornton et al., 2010; Mielke et al., 2016). During October-November 2014, Priestley et al. (2018) observed $ClNO_2$ persisting into the afternoon in Manchester, ∼120 km northwest of Leicester. However, in that study $ClNO_2$ decreased below the instrument detection limit (3.8 ppt) around 15:00, approximately 2 hours before sunset.

The conventional route for the formation of $ClNO_2$ requires the presence of N_2O_5 (Figure 1), which is formed by the reaction $NO_3 + NO_2$ and is mostly a nocturnal species. While N_2O_5 can sometimes be present during the day (Geyer et al., 2003; Brown et al., 2005; Osthoff et al., 2006), this is highly unlikely under the typical urban conditions of Europe. NO_3 photolyzes rapidly (with a lifetime of the order of 7-20 seconds at midday in winter) and reacts readily with NO: daytime urban mixing ratios of NO_x are in the order of tens of ppb (Bigi and Harrison, 2010), so the lifetime of NO_3 with respect to reaction with NO is $\leq$0.1 seconds (at the average winter temperature of 5 $^\circ$C), about an order of magnitude faster than the reaction of NO_3 with NO_2 to form N_2O_5. Therefore, NO_3 is effectively removed from the atmosphere before it can form N_2O_5, thus preventing formation of $ClNO_2$ during the day. There has been one prior report of daytime $ClNO_2$, with mixing ratios of $\sim$60 ppt observed in the afternoon in central China during summer (Liu et al., 2017). In order to explain their observations, Liu et al. (2017) proposed a photochemical mechanism involving very high mixing ratios of Cl_2 during the day (up to 450 ppt). However, such a mechanism cannot explain our observations of daytime $ClNO_2$ in Leicester, because Cl_2 was always below the instrument detection limit of 7.1 ppt.

Daytime production of $ClNO_2$ in Leicester can thus be ruled out, which might suggest that the observed daytime concentrations were instead caused by slower removal of $ClNO_2$ on the days when it persisted until sunset. However, this is not the case: the photolysis rates of $ClNO_2$ were similar in both cases (Figure 2), and actually slightly faster in the highCL case than in the lowCL case (by 5-7%, on average). If there was no $ClNO_2$ formation during the day and if the photolytic loss of $ClNO_2$ did not vary significantly, the only difference between the two cases was the amount of $ClNO_2$ present at sunrise (between 7:00 and 8:00 during winter). In fact, $ClNO_2$ concentrations at sunrise in the highCL case were, on average, 3.5 to 3.9 times higher than in the lowCL case, which, combined with the short days and slow photolysis rates of winter, resulted in the continuous presence of $ClNO_2$ throughout the day at mixing ratios of $>$10-20 ppt, i.e. a factor between of 2 and 5 times above the instrument detection limit (Figure 2). It must also be noted that the observed decay rate of $ClNO_2$ was, on average, within 10% of that calculated from the photolysis rates alone (Figure 4), which sug-

gests that deposition, heterogenous reactions and/or boundary layer dynamics did not have a significant effect on the variation of the $ClNO_2$ mixing ratio during the morning.

Both chemical and physical factors contribute to high mixing ratios of $ClNO_2$ at sunrise. Some studies (Thornton et al., 2010; McNamara et al., 2020; Wang et al., 2020) have suggested that snow and road salt can be sources of chloride during winter. However, this was not the case during this work, and the measurements of particulate chloride in Leicester during December 2014 (median concentration = 1.3 μg m^{-3}) were strongly correlated with sodium, indicating a marine origin (Sommariva et al., 2018). In fact, the analysis of the entire dataset showed that the chemical conditions for the formation of $ClNO_2$ in Leicester tend to be limited by the availability of O_3 rather than of NO_2 or chloride, especially during spring and winter (Sommariva et al., 2018). Generally, higher concentrations of ozone lead to stronger production of NO_3 and hence of N_2O_5, the key precursor of $ClNO_2$. However, this is not always the case and meteorological conditions can play a more important role than chemical conditions. Nights with higher $ClNO_2$ concentrations were usually colder (by 3-6 °C, Figure 2), which favours the thermal stability of N_2O_5; easterly winds (from less polluted areas of the UK) and stagnant meteorological conditions (wind speeds $<$2 m/s) also contributed to the accumulation of $ClNO_2$ during the night in the highCL case.

Previous studies in Northern Europe (Bannan et al., 2015; Priestley et al., 2018; Sommariva et al., 2018) have observed that $ClNO_2$ is typically present in urban environments during all seasons. Our measurements further show that, during winter, $ClNO_2$ often persists at significant mixing ratios (tens of ppt) through the daylight hours and thereby has the potential to provide a continuous source of Cl atoms in the urban boundary layer.

3.2. Effects on the production of radicals

The persistence of nitryl chloride from sunrise to sunset during winter days has two major effects on the formation of radicals in the urban atmosphere. First, more Cl atoms overall are released via $ClNO_2$ photolysis when $ClNO_2$ persists throughout the day (case highCL) than when it disappears around midday (case lowCL): this is a direct consequence of the higher concentrations of nitryl chloride at sunrise in the

highCL case (Figure 2). Figure 3 shows the average production rates and the total production of Cl and OH radicals. The average production rates of Cl peaked between 9:00 and 10:00 in the morning: the maximum Cl production rates were 3 to 10 times higher – and total Cl production was 3 to 8 times higher – in the highCL case compared to the lowCL case. Production of chlorine atoms was always higher in February than in December, because of the higher nocturnal $ClNO_2$ concentrations and faster diurnal photolysis rates (Figure 2).

Second, diurnal persistence of $ClNO_2$ affects the timing of the release of Cl atoms, and therefore of the production of O_3 and other secondary pollutants. One hour before sunset, which is at 16:00 in December and at 17:00 in February, the Cl production rates in the highCL case were 4 to 6 times higher than in the lowCL case. This means that production of chlorine atoms, and therefore oxidation of VOCs by Cl, remained significant ($> 1 \times 10^3$ atoms cm^{-3} s^{-1}) for most of the afternoon in the highCL case. While these values may seem small, it must be noted that VOC oxidation in winter is slower than in summer, due to the low concentrations of OH radicals and, therefore, even small increments in the amount of oxidants can impact the rates of formation of secondary pollutants.

To assess the impact of Cl on VOC oxidation, it is necessary to evaluate how it compares with the other main daytime oxidant, the OH radical, for which the dominant sources in an urban environment are the photolysis of O_3 and of HONO (Figure 1). HONO was not measured in Leicester, but HONO measurements were made in Birmingham in February 2014. Although these measurements were not contemporaneous with the $ClNO_2$ measurements made in Leicester, previous work has shown that HONO concentrations in the two locations are comparable (Crilley et al., 2016; Kramer et al., 2020). Therefore, we used the HONO data measured in Birmingham in February 2014 (Figure 2) as a proxy for HONO concentrations in Leicester in February 2016. The bimodal diurnal profile observed for HONO in Birmingham, peaking in the morning (07:00) and in the evening (18:00), suggests vehicle emissions are an important source (Kramer et al., 2020); the high nocturnal HONO mixing ratios ($\sim$150 ppt) point to nocturnal sources, likely heterogenous reactions of NO_2 on humid surfaces. The minimum HONO mixing ratio was observed at midday, with average mixing ratios of $\sim$65

ppt, which indicates sustained daytime source(s) that counteract the increased loss by photolysis.

The production rate of OH was calculated using the HONO measurements taken in Birmingham, together with the O_3 and photolysis rates measurements taken in Leicester. Figure 3 shows the average production rates and the total production of OH from O_3 and HONO photolysis during winter: OH production was dominated by HONO photolysis, which was 15-20 times larger than O_3 photolysis, consistent with other recent studies (Ren et al., 2006; Tan et al., 2018; Slater et al., 2020). Earlier studies (Emmerson et al., 2005; Kanaya et al., 2007) found instead that ozonolysis of unsaturated VOCs was the main primary source of OH in urban environments during winter: this issue will be discussed in the next section with the help of a box-model. The total production of OH and Cl (Figure 3, bottom) is the integrated number of OH molecules and Cl atoms per unit volume formed since sunrise. During the daylight hours, a total of $\sim 7.0 \times 10^{11}$ molecules cm^{-3} of OH radicals were formed from the photolysis of O_3 (5-7%) and of HONO (93-95%). By comparison, the total production of Cl atoms from $ClNO_2$ photolysis ranged between 1.3×10^9 atoms cm^{-3} (December, case lowCL) and 1.4×10^{11} atoms cm^{-3} (February, case highCL).

The calculations presented in Figure 3 show that, compared to the days with low concentrations of $ClNO_2$ at sunrise, the days with high concentrations of $ClNO_2$ at sunrise – which showed observable mixing ratios ($>$10-20 ppt) of $ClNO_2$ throughout the daylight hours – resulted in up to 8 times more Cl atoms activated in the gas phase, with production continuing at a significant rate right up until sunset. Moreover, the data show that substantial amounts of daytime HONO (in the order of a hundred ppt) were the source of almost all the OH radicals. In the following section, we discuss how these diurnal radical sources affect the oxidative processes in the wintertime urban boundary layer.

3.3. Effects on the oxidative capacity of the atmosphere

We used two approaches to understand the impact of continuous sources of radicals from the photolysis of $ClNO_2$ and HONO in winter and, hence, the relative importance of Cl and OH for the oxidation of VOCs. The following analysis focuses on the month

of February, for which both $ClNO_2$ and HONO measurements were available (Figure 2).

In the first approach, the lifetimes of selected VOCs were calculated for four different scenarios: with $ClNO_2$ persisting until sunset (highCL), with $ClNO_2$ disappearing by midday (lowCL), without $ClNO_2$ (noCL), without $ClNO_2$ and without daytime sources of HONO (noCL-HONO). The concentrations of OH and Cl used in this calculation were the values at 10:00 calculated with the box-model for the month of February, as discussed below. Table 2 shows that chlorine chemistry increases the oxidation rates of several VOCs, especially alkanes and oxygenated VOCs: comparing the lowCL and noCL scenarios, the lifetimes of VOCs decrease by between 4% (toluene) and 38% (propane). In the highCL scenario, when more Cl atoms overall are released (Figure 3), the lifetimes of VOCs further decrease by an additional 20% (isoprene) to 62% (propane) compared to the lowCL scenario. Of particular importance, because of its climate forcing role, is the effect of Cl on the lifetime of methane which decreases by between 7% (lowCL) and 36% (highCL), compared to the scenario where methane only reacts with OH (noCL). Alkenes, such as propene and isoprene, are less affected by the presence of chlorine (22-28% decrease in lifetimes in the highCL scenario compared to the noCL scenario) because they react with OH faster than alkanes and aromatics (Table 2).

The oxidation of the VOC pool is therefore significantly accelerated in the presence of $ClNO_2$. This is true in all seasons, but the effect is particularly pronounced under the unfavorable photochemical conditions of winter when other oxidant sources, such as O_3 photolysis, are weak. Moreover, the presence of daytime HONO sources leads to higher OH concentrations: if these sources were not taken into account (i.e. if HONO is only formed via OH + NO, as in scenario noCL-HONO), the calculated concentration of OH was 84% lower than the noCL scenario, with a corresponding increase in the lifetimes of VOCs (Table 2). Enhanced oxidation of VOCs affects the formation of gas-phase pollutants, such as O_3 (see below), and of secondary organic aerosol (SOA). Depending on the NO_x and humidity levels, SOA yields from isoprene and toluene oxidation vary between 1-5% and 10-30%, respectively (Ng et al., 2007; Carlton et al., 2009), which means that the increased oxidation of these VOCs can

result in additional SOA formation of up to ∼0.6% (from isoprene) and up to ∼9% (from toluene). Because of the differences in the rate coefficients of Cl with different VOCs, the actual impact of chlorine chemistry depends on the composition of the VOC mixture in the urban atmosphere. It must also be noted that chlorine reactivity has the potential to change the composition of the VOC pool, since some classes of compounds react more readily with Cl than with OH (Table 2).

The second approach used a simple box-model to calculate the effect of enhanced VOC oxidation rates on the production of secondary pollutants, particularly of ozone. The model was run for a 24h period under the four scenarios in Table 2: $ClNO_2$ was initialized using the mean observed $ClNO_2$ at sunrise in each scenario (Table 1). HONO was constrained to the average measured diurnal profiles in scenarios highCL, lowCL and noCL (Figure 2), and calculated by the model in scenario noCL-HONO. The box-model underestimated measured O_3 during the day by up to 4 ppb, because it only includes photochemical processes (rather than, e.g. mixing or transport); therefore, the following analysis is focused on the differences between the model scenarios.

The model results (Figure 4) show significant enhancements (a factor of ∼6) in the concentrations of Cl atoms in the highCL scenario compared to the lowCL scenario. Increased oxidation of VOCs by chlorine atoms also led to higher concentrations of OH (up to 30%), HO_2 and RO_2 (up to a factor of 2). The overall impact on the formation of secondary pollutants was significant, with increases of up to 22% and 57% in the concentrations of HCHO and CH_3CHO, respectively, and of up to 40% in the concentration of PAN compared to the noCL scenario. The increase in OH concentrations was most pronounced in the morning and was a consequence both of the higher concentrations of peroxy radicals and of the increased OH production from the photolysis of the oxygenated VOCs formed by the oxidation of primary VOCs. Figure 5 shows the amount of additional O_3 formed in the scenarios with $ClNO_2$ (highCL and lowCL) relative to the baseline scenario without $ClNO_2$ (noCL): between 0.13 ppb and 0.78 ppb more ozone was present at sunset due to Cl reactivity.

The model was also run for the month of December, but the impact of chlorine reactivity on secondary pollutant formation was more limited than in February: the additional ozone present at sunset in the highCL scenario was only ∼50 ppt compared

to the baseline scenario without chlorine chemistry (noCL). The main reason for the low impact of Cl is that both the concentrations and the photolysis rates of $ClNO_2$ were lower than in February (Figure 2), which resulted in $\sim$10 times less Cl atoms released across the day in December (Figure 3).

Analysis of the model results indicate that, in February, HONO was the primary source of OH in the urban boundary layer: the total production rate of OH in the middle of the day was 1.8×10^6 molecules cm^{-3} s^{-1}, of which 47% was due to recycling ($HO_2 + NO$), 45% due to HONO photolysis and only 5.5% due to O_3 photolysis, while the reactions of ozone with alkenes were responsible for less than 1% of the total OH production. These numbers are consistent with what can be directly inferred from our measurements (Figure 3), as well as with the studies by Ren et al. (2006); Tan et al. (2018); Slater et al. (2020). In contrast, early work in urban environments during winter (Emmerson et al., 2005; Kanaya et al., 2007) concluded that the ozonolysis of unsaturated VOCs was a source of OH radicals as large as HONO photolysis. The modelling study by Emmerson et al. (2005) is especially relevant, as it was conducted in Birmingham, the same region as this work: their model was also based on the MCM and included an heterogeneous HONO source in addition to the gas-phase reaction $OH + NO$, but it was not constrained to measured HONO, which raises the possibility that HONO concentrations were underestimated by the model. In fact, scenario noCL-HONO in Figure 4 shows that our model underestimated HONO concentrations by approximately a factor of 10 at 12:00 and a factor of 40 at 16:00, if not constrained to the observations of HONO. This resulted in lower OH concentrations (a factor of 4-5), as well as a shift in the peak OH concentration from 10:00 to 12:00 due to the low HONO concentrations in the morning. In the absence of a strong OH source – such as HONO photolysis – the model calculated that the O_3 concentration at sunset was 0.31 ppb less than in the baseline scenario noCL (Figure 5).

4. Conclusions

In this work, we discuss how the presence of strong sources of atomic chlorine, such as $ClNO_2$, in an urban environment during winter can substantially accelerate the

oxidation of VOCs resulting in the formation of additional ozone and other secondary pollutants (oxygenated VOCs, PAN and SOA).

Our observations show that, in winter, $ClNO_2$ can persist in significant mixing ratios (>10-20 ppt, on average) until sunset, and HONO can be present during the day at mixing ratios of the order of a hundred ppt. These conditions create sustained sources of Cl and OH radicals during all daylight hours, which enhance the oxidation of VOCs and extend the production of ozone and secondary pollutants in the afternoon. HONO photolysis dominates the formation of the OH radical, meaning that nitrous acid and nitryl chloride – rather than O_3 photolysis or ozonolysis of unsaturated VOCs – are the main sources of oxidants in the urban atmosphere during winter and are responsible for initiating most of the oxidative chemistry that forms atmospheric pollutants.

Multiple previous studies have shown that both $ClNO_2$ and HONO are present in a range of diverse environments and, hence, they are likely to play a fundamental role in wintertime urban photochemistry in other locations around the world. The processes that form $ClNO_2$ and HONO, however, are still highly uncertain and it is therefore recommended that future investigations focus on identifying and quantifying their sources, so that this chemistry can be accurately included in chemical models.

5. Acknowledgements

We thank the following for their help: D. Tanner, G. Huey (Georgia Institute of Technology); R. Leigh (University of Leicester); L. Kramer (University of Birmingham); G. Bustin, P. Chauhan, G. Nicholson, C. Schieferstein (University of Leicester Chemistry Workshop). Many thanks to J. Roberts (NOAA) for his continuing support and advice.

6. Funding

This work was supported by the UK Natural Environment Research Council [grant numbers: NE/K004069/1 and NE/M013545/1].

7. Tables

Table 1: Initial values of relative humidity (%), temperature (°C), inorganic species and VOCs (ppb) used in the box-model. HONO was constrained to its average measured diurnal profile in all scenarios, except in the noCL-HONO scenario where it was calculated by the model.
$^{(***)}$ scenario noCL-HONO only
$^{(**)}$ scenario highCL
$^{(*)}$ scenario lowCL

Species	Value	Species	Value
Relative Humidity	90	Temperature	5
O_3	20	trans-2-pentene	0.01
NO_x	15	cis-2-pentene	0.01
CO	140	1-pentene	0.01
CH_4	1900	2-methylpentane	0.07
ethane	6.30	isoprene	0.02
ethene	0.67	hexane	0.06
ethyne	0.49	heptane	0.03
propane	2.30	octane	0.02
propene	0.19	benzene	0.20
i-butane	0.59	toluene	0.19
n-butane	0.97	ethylbenzene	0.03
1-butene	0.05	m-xylene	0.05
trans-2-butene	0.02	p-xylene	0.05
cis-2-butene	0.02	o-xylene	0.04
i-pentane	0.30	1,2,3-trimethylbenzene	0.03
n-pentane	0.20	1,2,4-trimethylbenzene	0.05
1,3-butadiene	0.03	1,3,5-trimethylbenzene	0.02
$ClNO_2$ (Dec)	$0.07^{(**)}$ / $0.02^{(*)}$	HONO	$0.13^{(***)}$
$ClNO_2$ (Feb)	$0.31^{(**)}$ / $0.08^{(*)}$		

Table 2: Reaction rate coefficients of OH and Cl radicals with selected VOCs; lifetimes of selected VOCs with respect to reaction with OH and Cl radicals at 10:00 on February 15th. The concentrations of OH and Cl are in molecules or atoms cm^{-3}; the rate coefficients (Orlando et al., 2003; Smith et al., 2002; Atkinson et al., 2006) are in cm^3 $molecule^{-1}$ s^{-1} and are calculated for 5 °C (average winter temperature).

			Methane	Propane	Propene	Isoprene	Toluene	Ethanol
			CH_4	C_3H_8	C_3H_6	C_5H_8	C_7H_8	C_2H_5OH
		k_{OH}	4.2×10^{-15}	9.3×10^{-13}	3.1×10^{-11}	1.1×10^{-10}	6.1×10^{-12}	3.2×10^{-12}
		k_{Cl}	7.6×10^{-14}	1.4×10^{-10}	2.3×10^{-10}	4.3×10^{-10}	6.1×10^{-11}	1.0×10^{-10}
scenario	[OH]	[Cl]	VOCs lifetime (hours)					
highCL	6×10^5	1×10^4	84051	142	13	3.9	65	93
lowCL	5×10^5	2×10^3	122318	374	18	4.9	87	153
noCL	5×10^5	–	131127	600	18	5.0	91	172
noCL-HONO	8×10^4	–	819542	3747	113	31	568	1077

8. Figures

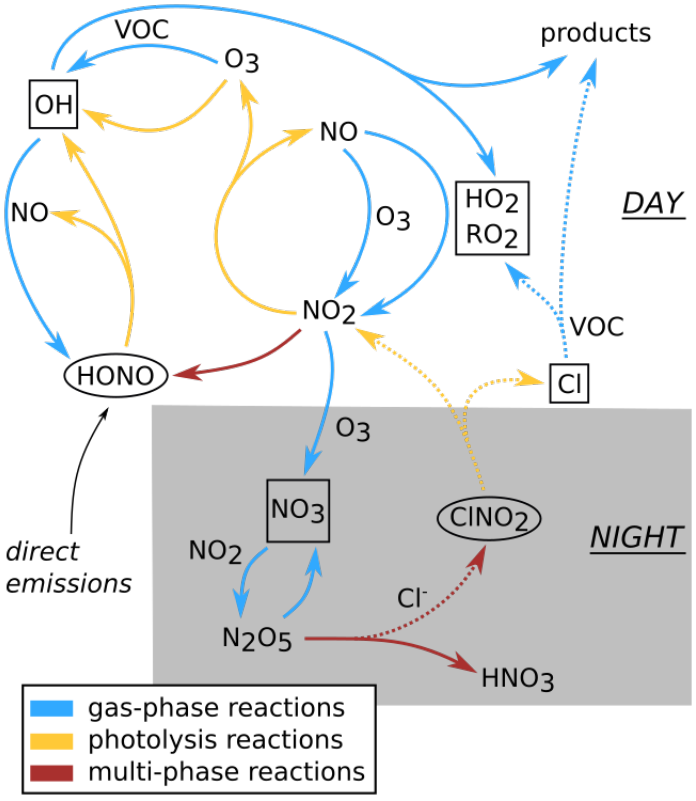

Figure 1: Scheme of the main chemical processes in the urban boundary layer. The dashed arrows indicate processes that require the presence of chloride-containing aerosol. The circles indicate the target species of this work ($ClNO_2$ and HONO) and the squares indicate the radical species.

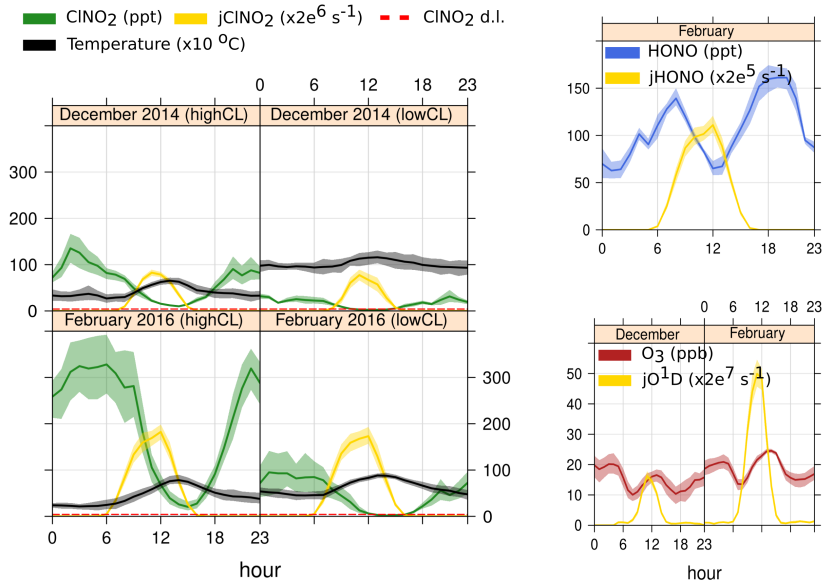

Figure 2: Average profiles of $ClNO_2$, O_3 and photolysis rates ($jClNO_2$, jO^1D, jHONO) measured in Leicester in December 2014 and February 2016; average profile of HONO measured in Birmingham in February 2014. The $ClNO_2$ and $jClNO_2$ data are divided into two cases: days when $ClNO_2$ remained above the detection limit all day (highCL) and days when $ClNO_2$ fell below the detection limit by midday (lowCL). The red dashed line shows the $ClNO_2$ detection limit (4.2 ppt) and the shading shows the 95% confidence intervals of the mean.

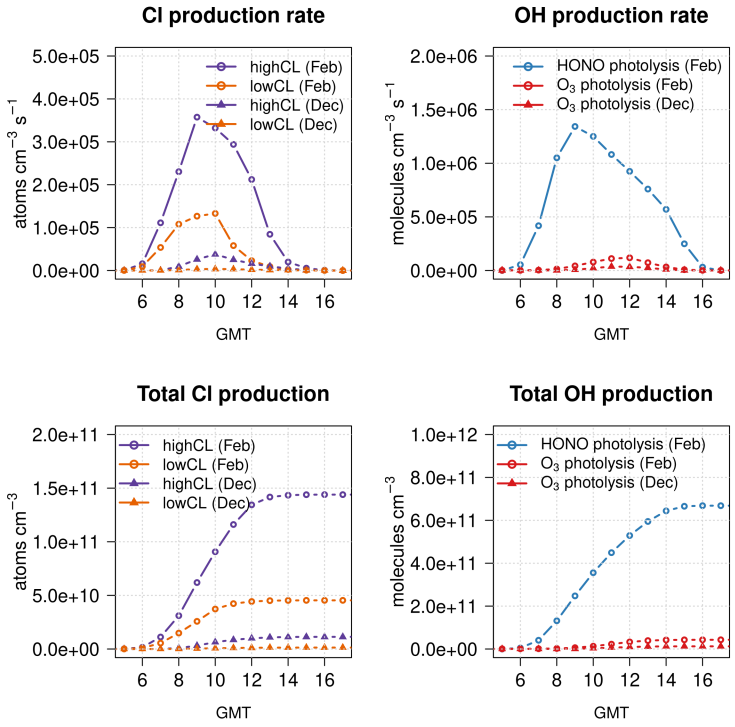

Figure 3: Average radical production rates (top) and total radical production (bottom) from O_3, HONO and $ClNO_2$ photolysis during winter.

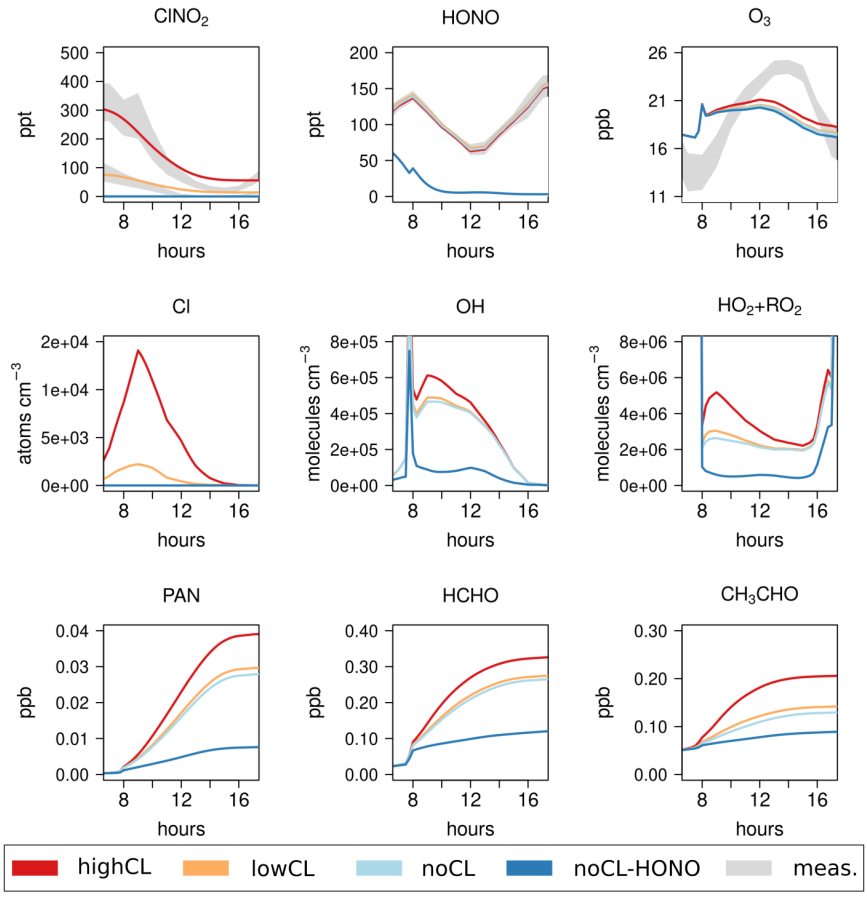

Figure 4: Results of the MCM box-model for the month of February, under the scenarios in Table 2. The grey shaded areas show the 95% confidence intervals of the mean for the observations of $ClNO_2$, HONO and O_3 (1-26 February 2016). Sunrise is at 7:30, sunset is at 17:00.

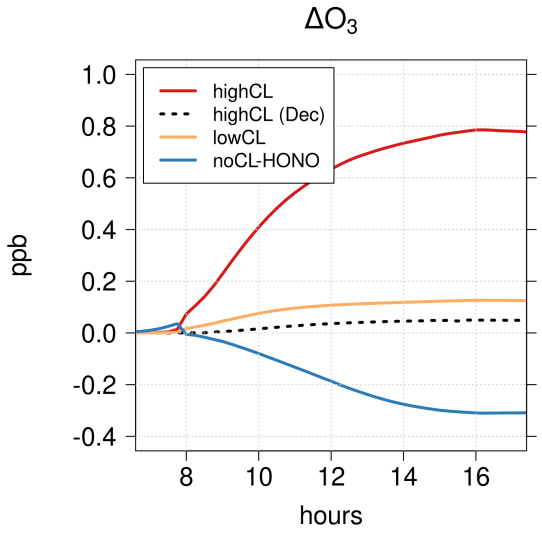

Figure 5: Difference between modelled ozone concentrations in each model scenario compared to the baseline scenario noCL (Table 2). Results are for the month February (unless indicated). Sunrise is at 7:30, sunset is at 17:00.

References

Ammann, M., Kalberer, M., Jost, D.T., Tobler, L., Rössler, E., Piguet, D., Gäggeler, H.W., Baltensperger, U., 1998. Heterogeneous production of nitrous acid on soot in polluted air masses. Nature 395, 157–160. doi:10.1038/25965.

Atkinson, R., Baulch, D.L., Cox, R.A., Crowley, J.N., Hampson, R.F., Hynes, R.G., Jenkin, M.E., Rossi, M.J., Troe, J., 2006. Evaluated kinetic and photochemical data for atmospheric chemistry: Volume II – gas phase reactions of organic species. Atmos. Chem. Phys. 6, 3625–4055. doi:10.5194/acp-6-3625-2006.

Baergen, A.M., Donaldson, D.J., 2016. Formation of reactive nitrogen oxides from urban grime photochemistry. Atmos. Chem. Phys. 16, 6355–6363. doi:10.5194/acp-16-6355-2016.

Bannan, T.J., Booth, A.M., Bacak, A., Muller, J.B.A., Leather, K.E., Le Breton, M., Jones, B., Young, D., Coe, H., Allan, J., Visser, S., Slowik, J.G., Furger, M., Prévôt, A.S.H., Lee, J., Dunmore, R.E., Hopkins, J.R., Hamilton, J.F., Lewis, A.C., Whalley, L.K., Sharp, T., Stone, D., Heard, D.E., Fleming, Z.L., Leigh, R., Shallcross, D.E., Percival, C.J., 2015. The first UK measurements of nitryl chloride using a chemical ionization mass spectrometer in central London in the summer of 2012, and an investigation of the role of Cl atom oxidation. J. Geophys. Res.: Atmos. 120, 5638–5657. doi:10.1002/2014JD022629.

Bigi, A., Harrison, R.M., 2010. Analysis of the air pollution climate at a central urban background site. Atmos. Environ. 44, 2004–2012. doi:10.1016/j.atmosenv.2010.02.028.

Brown, S.S., Osthoff, H.D., Stark, H., Dubé, W.P., Ryerson, T.B., Warneke, C., de Gouw, J.A., Wollny, A.G., Parrish, D.D., Fehsenfeld, F.C., Ravishankara, A.R., 2005. Aircraft observations of daytime NO_3 and N_2O_5 and their implications for tropospheric chemistry. J. Photochem. Photobiol., A 176, 270–278. doi:10.1016/j.jphotochem.2005.10.004.

458 Carlton, A.G., Wiedinmyer, C., Kroll, J.H., 2009. A review of secondary organic
459 aerosol (SOA) formation from isoprene. Atmos. Chem. Phys. 9, 4987–5005.
460 doi:10.5194/acp-9-4987-2009.

461 Chen, Q., Edebeli, J., McNamara, S.M., Kulju, K.D., May, N.W., Bertman, S.B.,
462 Thanekar, S., Fuentes, J.D., Pratt, K.A., 2019. HONO, particulate nitrite, and snow
463 nitrite at a midlatitude urban site during wintertime. ACS Earth Space Chem. 3,
464 811–822. doi:10.1021/acsearthspacechem.9b00023.

465 Crilley, L.R., Kramer, L., Pope, F.D., Whalley, L.K., Cryer, D.R., Heard, D.E., Lee,
466 J.D., Reed, C., Bloss, W.J., 2016. On the interpretation of in situ HONO observations
467 via photochemical steady state. Faraday Discuss. 189, 191–212. doi:10.1039/
468 c5fd00224a.

469 Elshorbany, Y.F., Kurtenbach, R., Wiesen, P., Lissi, E., Rubio, M., Villena, G.,
470 Gramsch, E., Rickard, A.R., Pilling, M.J., Kleffmann, J., 2009. Oxidation ca-
471 pacity of the city air of Santiago, Chile. Atmos. Chem. Phys. 9, 2257–2273.
472 doi:10.5194/acp-9-2257-2009.

473 Emmerson, K.M., Carslaw, N., Pilling, M.J., 2005. Urban atmospheric chemistry dur-
474 ing the PUMA campaign 2: radical budgets for OH, HO_2 and RO_2. J. Atmos. Chem.
475 52, 165–183. doi:10.1007/s10874-005-1323-2.

476 Finlayson-Pitts, B.J., Wingen, L.M., Sumner, A.L., Syomin, D., Ramazan, K.A., 2002.
477 The heterogeneous hydrolysis of NO_2 in laboratory systems and in outdoor and in-
478 door atmospheres: an integrated mechanism. Phys. Chem. Chem. Phys. 5, 223–242.
479 doi:10.1039/b208564j.

480 George, C., Strekowski, R.S., Kleffmann, J., Stemmler, K., Ammann, M., 2005. Pho-
481 toenhanced uptake of gaseous NO_2 on solid organic compounds: a photochemical
482 source of HONO? Faraday Discuss. 130, 195–210. doi:10.1039/b417888m.

483 Geyer, A., Alicke, B., Ackermann, R., Martinez, M., Harder, H., Brune, W., di Carlo,
484 P., Williams, E., Jobson, T., Hall, S., Shetter, R., Stutz, J., 2003. Direct observations

485 of daytime NO_3: implications for urban boundary layer chemistry. J. Geophys. Res.
486 108. doi:10.1029/2002jd002967.

487 Haskins, J.D., Lopez-Hilfiker, F.D., Lee, B.H., Shah, V., Wolfe, G.M., DiGangi, J.,
488 Fibiger, D., McDuffie, E.E., Veres, P., Schroder, J.C., Campuzano-Jost, P., Day,
489 D.A., Jimenez, J.L., Weinheimer, A., Sparks, T., Cohen, R.C., Campos, T., Sullivan,
490 A., Guo, H., Weber, R., Dibb, J., Green, J., Fiddler, M., Bililign, S., Jaeglé, L.,
491 Brown, S.S., Thornton, J.A., 2019. Anthropogenic control over wintertime oxidation
492 of atmospheric pollutants. Geophys. Res. Lett. 46, 14826–14835. doi:10.1029/
493 2019gl085498.

494 Heland, J., Kleffmann, J., Kurtenbach, R., Wiesen, P., 2001. A new instrument to
495 measure gaseous nitrous acid (HONO) in the atmosphere. Environ. Sci. Technol.
496 35, 3207–3212. doi:10.1021/es000303t.

497 Jenkin, M.E., Saunders, S.M., Wagner, V., Pilling, M.J., 2003. Protocol for the devel-
498 opment of the Master Chemical Mechanism, MCM v3 (Part B): tropospheric degra-
499 dation of aromatic volatile organic compounds. Atmos. Chem. Phys. 3, 181–193.
500 doi:10.5194/acp-3-181-2003.

501 Kanaya, Y., Cao, R., Akimoto, H., Fukuda, M., Komazaki, Y., Yokouchi, Y., Koike,
502 M., Tanimoto, H., Takegawa, N., Kondo, Y., 2007. Urban photochemistry in cen-
503 tral Tokyo: 1. Observed and modeled OH and HO_2 radical concentrations dur-
504 ing the winter and summer of 2004. J. Geophys. Res. 112. doi:10.1029/
505 2007JD008670.

506 Kleffmann, J., 2007. Daytime sources of nitrous acid (HONO) in the atmo-
507 spheric boundary layer. ChemPhysChem 8, 1137–1144. doi:10.1002/cphc.
508 200700016.

509 Kleffmann, J., Wiesen, P., 2008. Quantification of interferences of wet chemical
510 HONO LOPAP measurements under simulated polar conditions. Atmos. Chem.
511 Phys. 8, 6813–6822. doi:10.5194/acp-8-6813-2008.

Kramer, L.J., Crilley, L.R., Adams, T.J., Ball, S.M., Pope, F.D., Bloss, W.J., 2020. Nitrous acid (HONO) emissions under real-world driving conditions from vehicles in a UK road tunnel. Atmos. Chem. Phys. 20, 5231–5248. doi:10.5194/acp-20-5231-2020.

Kurtenbach, R., Becker, K.H., Gomes, J.A.G., Kleffmann, J., Lörzer, J.C., Spittler, M., Wiesen, P., Ackermann, R., Geyer, A., Platt, U., 2001. Investigations of emissions and heterogeneous formation of HONO in a road traffic tunnel. Atmospheric Environment 35, 3385–3394. doi:10.1016/s1352-2310(01)00138-8.

Lee, J.D., Whalley, L.K., Heard, D.E., Stone, D., Dunmore, R.E., Hamilton, J.F., Young, D.E., Allan, J.D., Laufs, S., Kleffmann, J., 2016. Detailed budget analysis of HONO in central London reveals a missing daytime source. Atmos. Chem. Phys. 16, 2747–2764. doi:10.5194/acp-16-2747-2016.

Liu, X., Qu, H., Huey, L.G., Wang, Y., Sjostedt, S., Zeng, L., Lu, K., Wu, Y., Hu, M., Shao, M., Zhu, T., Zhang, Y., 2017. High levels of daytime molecular chlorine and nitryl chloride at a rural site on the North China Plain. Environ. Sci. Technol. 51, 9588–9595. doi:10.1021/acs.est.7b03039.

McNamara, S.M., Kolesar, K.R., Wang, S., Kirpes, R.M., May, N.W., Gunsch, M.J., Cook, R.D., Fuentes, J.D., Hornbrook, R.S., Apel, E.C., China, S., Laskin, A., Pratt, K.A., 2020. Observation of road salt aerosol driving inland wintertime atmospheric chlorine chemistry. ACS Cent. Sci. 6, 684–694. doi:10.1021/acscentsci.9b00994.

Michoud, V., Colomb, A., Borbon, A., Miet, K., Beekmann, M., Camredon, M., Aumont, B., Perrier, S., Zapf, P., Siour, G., Ait-Helal, W., Afif, C., Kukui, A., Furger, M., Dupont, J.C., Haeffelin, M., Doussin, J.F., 2014. Study of the unknown HONO daytime source at a European suburban site during the MEGAPOLI summer and winter field campaigns. Atmos. Chem. Phys. 14, 2805–2822. doi:10.5194/acp-14-2805-2014.

Michoud, V., Doussin, J.F., Colomb, A., Afif, C., Borbon, A., Camredon, M., Aumont, B., Legrand, M., Beekmann, M., 2015. Strong HONO formation in a sub-

urban site during snowy days. Atmos. Environ. 116, 155–158. doi:10.1016/j.atmosenv.2015.06.040.

Mielke, L.H., Furgeson, A., Odame-Ankrah, C.A., Osthoff, H.D., 2016. Ubiquity of $ClNO_2$ in the urban boundary layer of Calgary, Alberta, Canada. Can. J. Chem. 94, 414–423. doi:10.1139/cjc-2015-0426.

Mielke, L.H., Furgeson, A., Osthoff, H.D., 2011. Observation of $ClNO_2$ in a mid-continental urban environment. Environ. Sci. Technol. 45, 8889–8896. doi:10.1021/es201955u.

Ng, N.L., Kroll, J.H., Chan, A.W.H., Chhabra, P.S., Flagan, R.C., Seinfeld, J.H., 2007. Secondary organic aerosol formation from m-xylene, toluene, and benzene. Atmos. Chem. Phys. 7, 3909–3922. doi:10.5194/acp-7-3909-2007.

Orlando, J.J., Tyndall, G.S., Apel, E.C., Riemer, D.D., Paulson, S.E., 2003. Rate coefficients and mechanisms of the reaction of Cl-atoms with a series of unsaturated hydrocarbons under atmospheric conditions. Int. J. Chem. Kinet. 35, 334–353. doi:10.1002/kin.10135.

Osthoff, H.D., Roberts, J.M., Ravishankara, A.R., Williams, E.J., Lerner, B.M., Sommariva, R., Bates, T.S., Coffman, D., Quinn, P.K., Dibb, J.E., Stark, H., Burkholder, J.B., Talukdar, R.K., Meagher, J., Fehsenfeld, F.C., Brown, S.S., 2008. High levels of nitryl chloride in the polluted subtropical marine boundary layer. Nat. Geosci. 1, 324–328. doi:10.1038/ngeo177. 13.

Osthoff, H.D., Sommariva, R., Baynard, T., Pettersson, A., Williams, E.J., Lerner, B.M., Roberts, J.M., Stark, H., Goldan, P.D., Kuster, W.C., Bates, T.S., Coffman, D., Ravishankara, A.R., Brown, S.S., 2006. Observation of daytime N_2O_5 in the marine boundary layer during New England Air Quality Study-Intercontinental Transport and Chemical Transformation 2004. J. Geophys. Res. 111. doi:10.1029/2006JD007593. 10.

Phillips, G.J., Tang, M.J., Thieser, J., Brickwedde, B., Schuster, G., Bohn, B., Lelieveld, J., Crowley, J.N., 2012. Significant concentrations of nitryl chloride

observed in rural continental Europe associated with the influence of sea salt chloride and anthropogenic emissions. Geophys. Res. Lett. 39. doi:10.1029/2012GL051912.

Priestley, M., le Breton, M., Bannan, T.J., Worrall, S.D., Bacak, A., Smedley, A.R.D., Reyes-Villegas, E., Mehra, A., Allan, J., Webb, A.R., Shallcross, D.E., Coe, H., Percival, C.J., 2018. Observations of organic and inorganic chlorinated compounds and their contribution to chlorine radical concentrations in an urban environment in northern Europe during the wintertime. Atmos. Chem. Phys. 18, 13481–13493. doi:10.5194/acp-18-13481-2018.

Ren, X., Brune, W.H., Mao, J., Mitchell, M.J., Lesher, R.L., Simpas, J.B., Metcalf, A.R., Schwab, J.J., Cai, C., Li, Y., 2006. Behavior of OH and HO_2 in the winter atmosphere in New York City. Atmos. Environ. 40, 252–263. doi:10.1016/j.atmosenv.2005.11.073.

Riedel, T.P., Bertram, T.H., Crisp, T.A., Williams, E.J., Lerner, B.M., Vlasenko, A., Li, S.M., Gilman, J., de Gouw, J., Bon, D.M., Wagner, N.L., Brown, S.S., Thornton, J.A., 2012. Nitryl chloride and molecular chlorine in the coastal marine boundary layer. Environ. Sci. Technol. 46, 10463–10470. doi:10.1021/es204632r.

Sarwar, G., Simon, H., Xing, J., Mathur, R., 2014. Importance of tropospheric $ClNO_2$ chemistry across the Northern Hemisphere. Geophys. Res. Lett. 41, 4050–4058. doi:10.1002/2014GL059962.

Saunders, S.M., Jenkin, M.E., Derwent, R.G., Pilling, M.J., 2003. Protocol for the development of the Master Chemical Mechanism, MCM v3 (Part A): tropospheric degradation of non-aromatic volatile organic compounds. Atmos. Chem. Phys. 3, 161–180. doi:10.5194/acp-3-161-2003.

Sherwen, T., Evans, M.J., Sommariva, R., Hollis, L.D.J., Ball, S.M., Monks, P.S., Reed, C., Carpenter, L.J., Lee, J.D., Forster, G., Bandy, B., Reeves, C.E., Bloss, W.J., 2017. Effects of halogens on European air-quality. Faraday Discuss. 200, 75–100. doi:10.1039/c7fd00026j. 29.

Simpson, W.R., Brown, S.S., Saiz-Lopez, A., Thornton, J.A., von Glasow, R., 2015. Tropospheric halogen chemistry: sources, cycling, and impacts. Chem. Rev. 115, 4035–4062. doi:10.1021/cr5006638.

Slater, E.J., Whalley, L.K., Woodward-Massey, R., Ye, C., Lee, J.D., Squires, F., Hopkins, J.R., Dunmore, R.E., Shaw, M., Hamilton, J.F., Lewis, A.C., Crilley, L.R., Kramer, L., Bloss, W., Vu, T., Sun, Y., Xu, W., Yue, S., Ren, L., Acton, W.J.F., Hewitt, C.N., Wang, X., Fu, P., Heard, D.E., 2020. Elevated levels of OH observed in haze events during wintertime in central Beijing. Atmos. Chem. Phys. 20, 14847–14871. doi:10.5194/acp-20-14847-2020.

Smith, J.D., DeSain, J.D., Taatjes, C.A., 2002. Infrared laser absorption measurements of HCl(v=1) production in reactions of Cl atoms with isobutane, methanol, acetaldehyde, and toluene at 295 K. Chem. Phys. Lett. 366, 417–425. doi:10.1016/s0009-2614(02)01621-4.

Sommariva, R., Cox, S., Martin, C., Borońska, K., Young, J., Jimack, P.K., Pilling, M.J., Matthaios, V.N., Nelson, B.S., Newland, M.J., Panagi, M., Bloss, W.J., Monks, P.S., Rickard, A.R., 2020. AtChem (version 1), an open-source box model for the Master Chemical Mechanism. Geosci. Model Dev. 13, 169–183. doi:10.5194/gmd-13-169-2020. 33.

Sommariva, R., Hollis, L.D.J., Sherwen, T., Baker, A.R., Ball, S.M., Bandy, B.J., Bell, T.G., Chowdhury, M.N., Cordell, R.L., Evans, M.J., Lee, J.D., Reed, C., Reeves, C.E., Roberts, J.M., Yang, M., Monks, P.S., 2018. Seasonal and geographical variability of nitryl chloride and its precursors in Northern Europe. Atmos. Sci. Lett. 19. doi:10.1002/asl.844. 30.

Spataro, F., Ianniello, A., 2014. Sources of atmospheric nitrous acid: state of the science, current research needs, and future prospects. J. Air Waste Manage. Assoc. 64, 1232–1250. doi:10.1080/10962247.2014.952846.

Stemmler, K., Ammann, M., Donders, C., Kleffmann, J., George, C., 2006. Photosensitized reduction of nitrogen dioxide on humic acid as a source of nitrous acid. Nature 440, 195–198. doi:10.1038/nature04603.

626 Su, H., Cheng, Y., Oswald, R., Behrendt, T., Trebs, I., Meixner, F.X., Andreae, M.O.,
627 Cheng, P., Zhang, Y., Poschl, U., 2011. Soil nitrite as a source of atmospheric HONO
628 and OH radicals. Science 333, 1616–1618. doi:10.1126/science.1207687.

629 Tan, Z., Rohrer, F., Lu, K., Ma, X., Bohn, B., Broch, S., Dong, H., Fuchs, H., Gkatzelis,
630 G.I., Hofzumahaus, A., Holland, F., Li, X., Liu, Y., Liu, Y., Novelli, A., Shao, M.,
631 Wang, H., Wu, Y., Zeng, L., Hu, M., Kiendler-Scharr, A., Wahner, A., Zhang, Y.,
632 2018. Wintertime photochemistry in Beijing: observations of RO_x radical concen-
633 trations in the North China Plain during the BEST-ONE campaign. Atmos. Chem.
634 Phys. 18, 12391–12411. doi:10.5194/acp-18-12391-2018.

635 Thaler, R.D., Mielke, L.H., Osthoff, H.D., 2011. Quantification of nitryl chloride at
636 part per trillion mixing ratios by thermal dissociation cavity ring-down spectroscopy.
637 Anal. Chem. 83, 2761–2766. doi:10.1021/ac200055z.

638 Thalman, R., Baeza-Romero, M.T., Ball, S.M., Borrás, E., Daniels, M.J.S., Goodall,
639 I.C.A., Henry, S.B., Karl, T., Keutsch, F.N., Kim, S., Mak, J., Monks, P.S., Muñoz,
640 A., Orlando, J., Peppe, S., Rickard, A.R., Ródenas, M., Sánchez, P., Seco, R.,
641 Su, L., Tyndall, G., Vázquez, M., Vera, T., Waxman, E., Volkamer, R., 2015.
642 Instrument intercomparison of glyoxal, methyl glyoxal and NO_2 under simulated
643 atmospheric conditions. Atmos. Meas. Tech. 8, 1835–1862. doi:10.5194/
644 amt-8-1835-2015.

645 Tham, Y.J., Wang, Z., Li, Q., Yun, H., Wang, W., Wang, X., Xue, L., Lu, K., Ma,
646 N., Bohn, B., Li, X., Kecorius, S., Größ, J., Shao, M., Wiedensohler, A., Zhang,
647 Y., Wang, T., 2016. Significant concentrations of nitryl chloride sustained in the
648 morning: investigations of the causes and impacts on ozone production in a polluted
649 region of northern China. Atmos. Chem. Phys. 16, 14959–14977. doi:10.5194/
650 acp-16-14959-2016.

651 Thornton, J.A., Kercher, J.P., Riedel, T.P., Wagner, N.L., Cozic, J., Holloway, J.S.,
652 Dubé, W.P., Wolfe, G.M., Quinn, P.K., Middlebrook, A.M., Alexander, B., Brown,
653 S.S., 2010. A large atomic chlorine source inferred from mid-continental reactive
654 nitrogen chemistry. Nature 464, 271–274. doi:10.1038/nature08905.

Villena, G., Kleffmann, J., Kurtenbach, R., Wiesen, P., Lissi, E., Rubio, M.A., Croxatto, G., Rappenglück, B., 2011. Vertical gradients of HONO, NO_x and O_3 in Santiago de Chile. Atmos. Environ. 45, 3867–3873. doi:10.1016/j.atmosenv.2011.01.073.

Vogel, B., Vogel, H., Kleffmann, J., Kurtenbach, R., 2003. Measured and simulated vertical profiles of nitrous acid – Part II. Model simulations and indications for a photolytic source. Atmos. Environ. 37, 2957–2966. doi:10.1016/S1352-2310(03)00243-7.

Wang, S., McNamara, S.M., Kolesar, K.R., May, N.W., Fuentes, J.D., Cook, R.D., Gunsch, M.J., Mattson, C.N., Hornbrook, R.S., Apel, E.C., Pratt, K.A., 2020. Urban snowpack $ClNO_2$ production and fate: a one-dimensional modeling study. ACS Earth Space Chem. 4, 1140–1148. doi:10.1021/acsearthspacechem.0c00116.

Wang, T., Tham, Y.J., Xue, L., Li, Q., Zha, Q., Wang, Z., Poon, S.C.N., Dubé, W.P., Blake, D.R., Louie, P.K.K., Luk, C.W.Y., Tsui, W., Brown, S.S., 2016. Observations of nitryl chloride and modeling its source and effect on ozone in the planetary boundary layer of southern China. J. Geophys. Res.: Atmos. 121, 2476–2489. doi:10.1002/2015JD024556.

Wang, X., Jacob, D.J., Eastham, S.D., Sulprizio, M.P., Zhu, L., Chen, Q., Alexander, B., Sherwen, T., Evans, M.J., Lee, B.H., Haskins, J.D., Lopez-Hilfiker, F.D., Thornton, J.A., Huey, G.L., Liao, H., 2019. The role of chlorine in global tropospheric chemistry. Atmos. Chem. Phys. 19, 3981–4003. doi:10.5194/acp-19-3981-2019.